Bench-Scale Test Facility for Evaluating the Performance of Thermal Imagers for Fire Service Applications

Sung Chan Kim[1] and Anthony Hamins[2]*

1. Department of Fire Safety, Kyungil University, 50 Gamasil-gil, Hayang-eup, Gyeongsan, Gyeongbuk, 38428, Republic of Korea
2. National Insitute of Standards and Technology, 100 Bureau Drive, Mail Stop 8664, Gaithersburg, MD 20899 USA

ABSTRACT

A bench-scale facility was developed for the evaluation of thermal imaging cameras. Smoke obscuration conditions in the optical smoke cell were characterized by measuring laser light transmittance through the cell. Measurements showed that the laser transmittance along the axial direction of the optical smoke cell was relatively uniform in the upper and lower halves of the cell for various smoke obscuration conditions. The thermal sensitivity of thermal imagers was investigated using the Michelson Contrast (CM) as a performance metric for a bar target viewed through the smoke-filled cell for different background thermal conditions. The results of the study indicate that the optical smoke cell can be utilized as a well-controlled and effective bench-scale test apparatus to evaluate aspects of the performance of thermal imagers for fire service applications.

KEYWORDS: Bench Scale Test, Infrared, Laser Transmittance, Thermal Imager, Fire Fighting

* corresponding author: (Email: anthony.hamins@nist.gov)

Introduction

The applications of thermal imaging devices using infrared (IR) sensors are almost endless, ranging from simple temperature measurements to IR signature analysis, tracking applications, medical usage, and even measurement of mechanical stress [1,2]. In the fire service, thermal imagers have emerged as one of the most technologically advanced tools for increasing safety and efficiency [3,4]. Visibility in real fire situations is greatly reduced not only by heavy smoke and water vapor but also by electrical blackouts due to fire. For these reasons, IR technology offers an alternative view of the fire scene, allowing fire fighters to see a fire and hazardous spots through smoke. Thermal imagers are also being used for search and rescue of victims, identifying hot spots, locating escape routes, and tracking fire growth. Although thermal imagers provide many benefits to the fire service, there is currently no standard quantitative methodology that considers performance under realistic conditions such as environments characterized as smoke laden and filled with combustion products. This study presents a test method for evaluating infrared thermal imaging cameras, and provides an understanding of key factors that affect imaging performance [5,6].

Infrared cameras are able to image objects through combustion gases, yet smoke and soot attenuate the target signal. Recently, there have been a number of studies concerned with imager performance in fire conditions to characterize imager performance looking at a hot surface. Sudheer and Prabhu considered the effects of the emissivity of gasoline pool flames on the images acquired by a microbolometer detector looking at a well characterized target behind the flames [7]. In another study, these authors used a heated blackbody to measure emissivities of various hydrocarbon flames [8]. De Vries and Tabinowski [9] investigated the performance of IR cameras measuring surface temperatures through ethylene and propane flames. These studies considered effects associated with high temperature flame emission and there was less concern about the post-flame (and colder) smoke on imager performance.

To evaluate imager performance under realistic fire conditions, large-scale or bench-scale tests can be conducted. Large-scale tests are expensive, time consuming, hazardous, and typically have poor reproducibility. Reproducibility of test conditions is an important factor for reliable performance evaluation. Bench-scale tests are typically more controlled, convenient, inexpensive, quick and provide more consistent results than large-scale tests. In 2009, the National Fire Protection Association (NFPA) released 'NFPA1801: Standard on Thermal Imagers for the Fire Service' to evaluate the performance of thermal imaging cameras for fire fighting applications [10]. This standard contains well-characterized bench-scale tests of imaging performance such as image recognition, thermal contrast, and thermal sensitivity, which are important for the characterization of various aspects of imager performance. It is also important to consider imager performance under fire conditions, including the presence of smoke particulates [11,12].

This study is focused on the performance of thermal imagers under conditions that are not unlike those experienced by fire fighters during search and rescue when relatively cool smoke (rather than "hot" combusting flames) are present in the field of view. Understanding the smoke effects can help characterize thermal imagers. A bench-scale test facility was developed that includes smoke from the burning of a well-characterized gaseous fuel, propene (or propylene). Propene was selected as the fuel since it yields copious amounts of soot relative to many gaseous hydrocarbons. Measurements were performed to investigate the performance of the facility in evaluating key aspects of the performance of thermal imagers. The conditions inside the optical smoke cell were characterized with emphasis on the Michelson Contrast (C_M) function, which was used to quantitatively assess image quality.

EXPERIMENT

Optical Smoke Cell and Premixed Chimney Burner

Figure 1 shows a schematic of the optical smoke cell, which was developed to simulate a smoky fire environment. A brass cylinder of 12.7 cm in diameter and 30.5 cm in length was used as the main body of the cell. Nitrogen purge streams flowed across the inner faces of the windows at each end of the main cell body. The smoke inlets were connected at the bottom of the main body of the smoke cell; the outlets were positioned at the mid-section of the main body. The outlet flows from the smoke cell were connected to a 5 cm diameter tube and exhausted into the laboratory hood, such that the pressure inside the cell was ambient. The gas temperature at the inlet, outlet, and three positions inside the optical smoke cell was measured with J-type thermocouples.

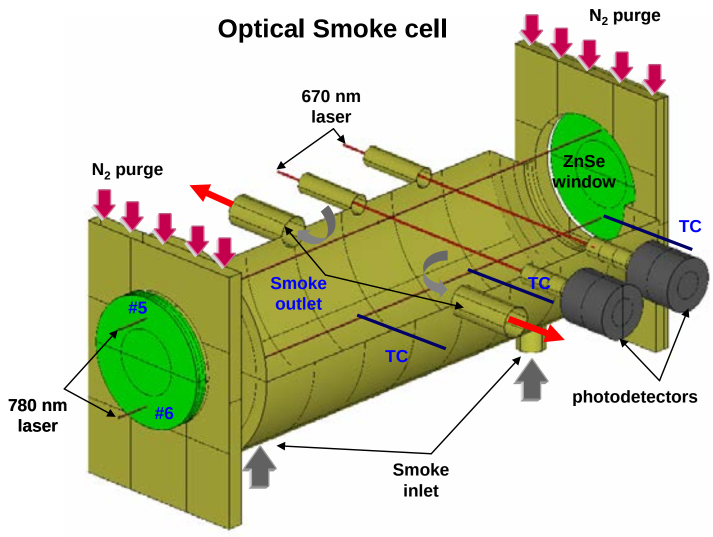

Figure 1. Schematic of the optical smoke cell with laser transmission measurement through the smoky media in the axial and transverse directions. The chimney burner is shown on the right.

To characterize the test conditions, laser transmission measurements were conducted through the media in both the axial and transverse directions within the optical smoke cell. The medial and axial laser light sources were continuous wave diode lasers at 670 nm and 780 nm wavelength, respectively. The detectors were silicon photodiodes sensitive from 350 nm to 1100 nm. Narrow, bandpass wavelength filters (10 nm) were placed in front of each of the detectors. In the transverse direction, a guide tube with a nitrogen purge flow of 150 ml/min was connected to the main cell body and a glass window of 1.3 cm diameter was attached at each end of the guide tube. To reduce beam-steering effects, diffusing filters were used to expand the transmitted laser beam in front of the detectors. The transmitted light signal was recorded at 5 Hz using a data acquisition system (DAQ). The laser transmittance at a specified wavelength (τ_λ) through the optical smoke cell is the ratio of the attenuated intensity (I_λ) to the reference intensity ($I_{o,\lambda}$).

$$\tau_\lambda = \frac{I_\lambda}{I_{o,\lambda}} \tag{1}$$

The reference intensity was obtained by averaging during a period of 60 s before introducing smoke media. Beam splitters were installed in front of each laser allowing monitoring of the unperturbed laser signal to provide a correction to the reference intensity for the transmission measurement.

The absorbance (α_λ) is defined as the logarithm of the reciprocal of the transmittance at the specified wavelength.

$$\alpha_\lambda = \log\left(\frac{1}{\tau_\lambda}\right) \tag{2}$$

The light-extinction coefficient (κ) is defined in terms of the laser transmittance passing through the smoke with path length (L) [13]:

$$\kappa = -\frac{\ln(\tau_\lambda)}{L} \tag{3}$$

The smoke density based on a light-extinction measurement is estimated as follows:

$$m_s = \frac{\kappa}{\sigma_s} \tag{4}$$

where σ_s is the mass-specific extinction coefficient. The present study assumes the constant mass specific extinction coefficient of 8.7 m^2/g ± 5.4 % for flame generated smoke although the value greatly depends on the fuel type, combustion conditions, and other factors [14].

All uncertainties are presented as the expanded combined uncertainty (2σ), which is the square root of the sum of the individual uncertainties associated with the terms that influence the light-extinction measurement and its variance.

Zinc selenide (ZnSe) windows with a diameter of 7.6 cm were installed on either end of the smoke cell to allow transmission of infrared radiation. For visible camera tests, glass windows were used instead of ZnSe. A 45 L/min nitrogen purge stream was used to protect these sensitive windows from smoke deposition and heat.

A chimney burner and heated tubing were used to generate smoke, which flowed into the smoke cell. Propene (C_3H_6) and air formed a premixed flame in the burner, from which the smoke and combustion gas concentrations were controlled by varying the air and fuel volumetric flow rates. A constant fuel flow of 0.6 l/min was mixed with a range of air flows (from 2.4 l/min to 5.4 l/min) such that the ratio of the volumetric flows of air to fuel varied from 4 to 9. The chimney and tube walls were wrapped with electrically controlled heating tape to maintain the gas temperature at 140 °C at the smoke cell inlets.

Test Apparatus

Figure 2 (a) shows a schematic of the bench-scale test facility, which facilitated evaluation of the image quality of thermal imagers. The facility consisted of three main parts - the first is the target and background, the second is the optical smoke cell, and the last is the thermal imager. The target was made with 2.3 cm diameter copper tubing covered with an optical black coating having an emissivity of 0.94 in the spectral range of 0.3 µm to 15 µm The target temperature was maintained at 30±1.2 °C using circulating ethylene glycol. The background was an extended rectangular area blackbody, 10 cm in each dimension. The emissivity of the blackbody was 0.97±0.02 and the absolute temperature range was from 0 °C to 175 °C with a measured temperature uniformity of ±0.015 °C. A 15.2 cm diameter spherical mirror with a focal length of 61 cm was used to project the radiation from the target onto the thermal imager.

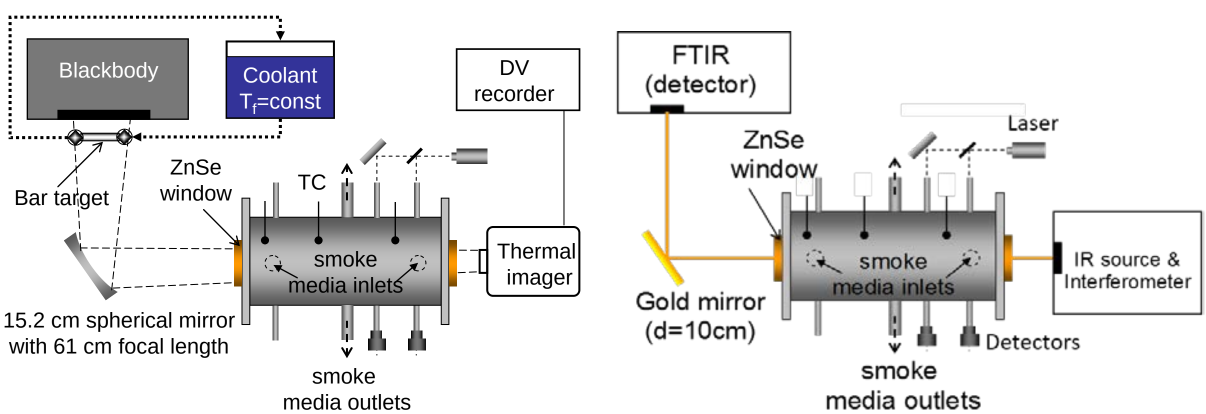

(a) Image quality characterization mode (b) Smoke property characterization mode

Figure 2. Schematic of the bench-scale test facility for image quality measurements of a thermal imager and smoke measurements for characterization of the optical smoke cell contents.

Before image quality tests of the thermal imaging cameras, quantitative measurement of combustion products inside the optical smoke cell was investigated using Fourier Transform Infrared Spectrometer

(FTIR) gas measurement system, used in the transmission (or active) mode. The resolution of the FTIR measurement was 0.25 cm^{-1}. For these measurements, the thermal imager and target-background of the image quality measurement setup were replaced with the FTIR source and detector, respectively, as shown in Figure 2 (b).

Table 1 summarizes the three types of thermal imagers tested. The sensor types were Barium-Strontium-Titanate (BST), Amorphous Silicon (ASi), and a Vanadium Oxide (VOx) micro-bolometer. The detectors operated in the spectral range from about 8 µm to 14 µm with plane array detectors of 320×240 pixels for the BST and VOx technologies and 160×120 pixels for ASi, respectively. The focal length was set from 1 m to infinity and the field of view ranged from 34° to 55° in the horizontal direction and 26° to 55° in the vertical direction. Long wavelength, thermal imaging cameras were selected for the ability to target and image through smoke and soot.

Table 1. Summary of thermal imaging camera specifications

Imager / Characteristics	TIC A	TIC B	TIC C
Sensor type	BST	ASi	VOx
Spectral Response	8~14 μm	7½ ~14 μm	8-14 μm
Field of View	55°	Horizontal: 37.5° Vertical: 50°	Horizontal: 34° Vertical: 26°
Focal Length	> 1 m	> 1m	> 1m
Array size	320×240	160×120	320×240

Figure 3 shows the overall procedure to test the image quality using the optical smoke cell. The test procedure included two stages. The first characterized the smoke conditions inside of the optical smoke cell by temperature, light-extinction, and FTIR measurement. The second characterized the image quality through the smoke in the optical cell, considering the camera's image contrast for various background and target surface temperature conditions. The images taken by the thermal imager were recorded using a digital video recorder. The captured digital video was analyzed with NI-IMAQ (National Instruments-Image Acquisition) vision software.

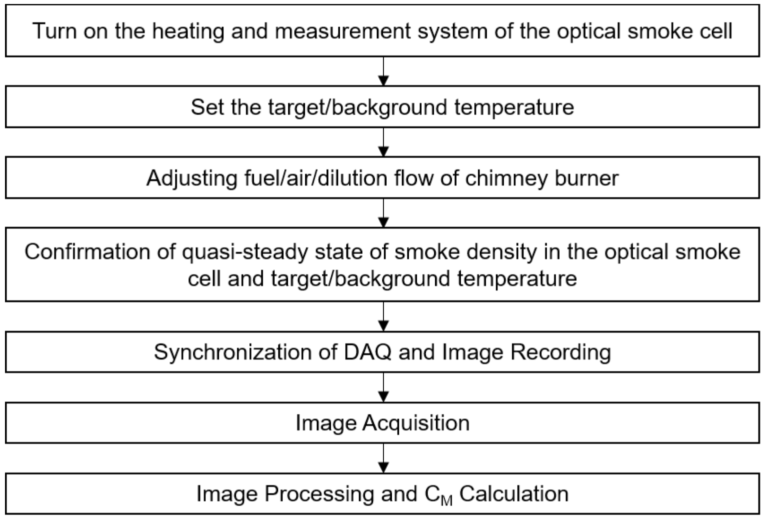

Figure 3. Procedure to test the image quality of thermal imager by using the optical smoke cell.

RESULTS AND DISCUSSION

Smoke Characterization of the Optical Smoke Cell

Figure 4 shows the transmittance of the laser beam along the axial direction through the upper and lower halves of the optical smoke cell filled with combustion products. The fuel volumetric flow rate was held constant at 0.6 l/min, while the air volumetric flow rate was increased from 2.4 l/min to 5.4 l/min.

The smoke density inside the optical smoke cell depended on the combustion conditions in the chimney burner and the total flow rate of combustion products. The stoichiometric (volumetric) air to fuel ratio of propene is about 21.4. Testing was conducted with the chimney burner set for global equivalence ratios (φ) from about 4 to 9, facilitating controlled introduction of smoke into the test cell. Figure 4 shows that the intensity of transmitted light continuously decreased until it was almost constant for air flow rates greater than 4.2 l/min. For these fuel rich conditions, repeatable laser light transmittance (τ_λ) measurements through the smoke, varying from about 0.1 to 1, were obtained. The overall laser light-extinction coefficient along the lower section of the optical smoke cell was within 10 % of the upper section.

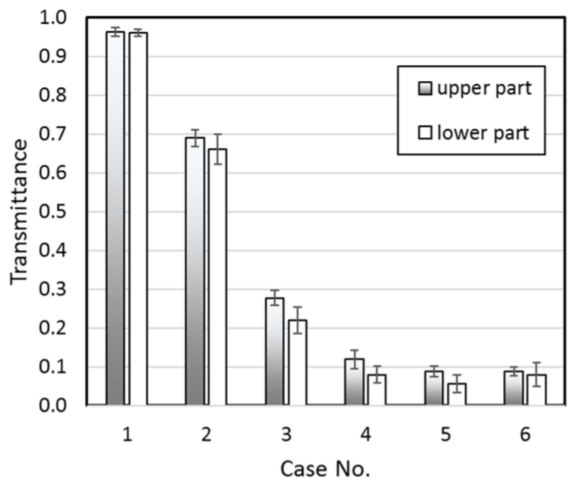

Figure 4. The averaged transmittance measured using a 780 nm laser in the axial direction through the upper and lower halves of the optical cell for various air flow rates at a constant fuel flow (0.6 l/min). The error bars represent one standard deviation based on repeat measurements.

Table 2 summarizes the mean transmittance along the axial direction through the optical smoke cell for various conditions characterized by the values of the fuel and air flows. For simplification, the present study categorizes test conditions based on the transmittance of the laser beam along the axial direction of the optical smoke cell. Here, Class I is defined as transmittance larger than 0.6, Class II as transmittance between 0.1 and 0.6, and Class III as transmittance less than 0.1.

Table 2 Smoke obscuration based on the mean transmittance in the axial direction through the optical smoke cell for various fuel and air flow rate

<table>
<tr><th>Case</th><th>Total volumetric flow rate (L/min)</th><th>Transmittance</th><th>Smoke condition</th></tr>
<tr><td>1</td><td>3.0</td><td>0.964 ± 0.021</td><td rowspan="2">Class I</td></tr>
<tr><td>2</td><td>3.6</td><td>0.675 ± 0.046</td></tr>
<tr><td>3</td><td>4.2</td><td>0.253 ± 0.043</td><td>Class II</td></tr>
<tr><td>4</td><td>4.8</td><td>0.109 ± 0.030</td><td rowspan="3">Class III</td></tr>
<tr><td>5</td><td>5.4</td><td>0.084 ± 0.024</td></tr>
<tr><td>6</td><td>6.0</td><td>0.072 ± 0.030</td></tr>
</table>

Figure 5 shows the captured visible images through the optical smoke cell during the test for different levels of smoke obscuration. For Class I conditions, the bar target was clearly distinguished through the smoke and the scattered light from the laser beam was observed. For Class II conditions, the bar target was hardly distinguished through the smoke. For Class III conditions, the optical cell was filled with copious amounts of smoke and the bar target could not be distinguished.

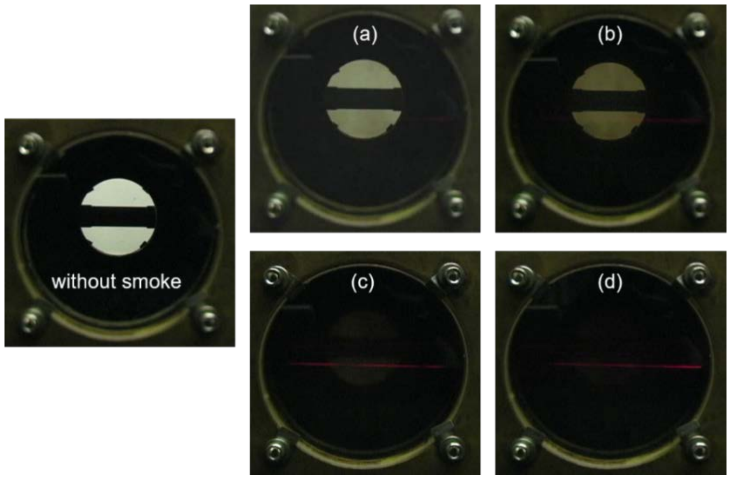

Figure 5. Comparison of the visible images through the optical smoke cell for various smoke conditions (a) Class I conditions with transmittance higher than 0.9 (b) Class I conditions with transmittance between 0.6 and 0.7 (c) Class II conditions with transmittance between 0.2 and 0.3 (d) Class III conditions with transmittance less than 0.1.

The contrast is a commonly used quantitative parameter to distinguish the target from background of an image. Among the various measures of contrast, the present study uses the Michelson contrast [15] function, which is defined as follows:

$$C_M = \frac{J_{\max} - J_{\min}}{J_{\max} + J_{\min}} \tag{5}$$

where $J_{\max}$ and $J_{\min}$ are the highest and lowest values of the intensity in the region of the target and the background. Figure 6 represents the spatial luminance for the different quality of the images. The gray image transferred from the captured image is 8 bit and the luminance intensity ranged between 0 and 255 (2^8) according to its brightness. By definition, the value of C_M can vary from 0 to 1 with the minimum indicating that there is no contrast and the maximum indicating the highest contrast.

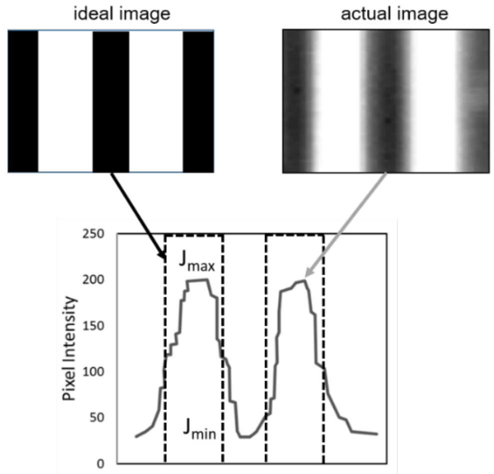

Figure 6. Spatial pixel luminance for ideal contrast (dotted line) and a representative image with target and background (solid line).

A simple visibility model based on the light-extinction coefficient and target characteristics through the smoke was proposed by Jin: [16]

$$S = C \cdot \kappa^{-1} \tag{6}$$

The visibility (S) is taken as inversely proportional to the light-extinction coefficient. The constant C mainly depends on target characteristics such as the reflectance of a sign and the brightness threshold of illuminating light; its value is almost constant for a given target/sign lighting condition. Taking the constant C in Eq. 6 as equal to 8, which is typical for a light-emitting target [17], the visibility of the test conditions ranged between 0.9 m and 62 m. When the visibility is smaller than 2 m, conditions typically drop below the lower tenability limit for life safety [18].

C_M can be thought of as analogous to S in Eq. 6, representative of target visibility through a smoke-filled environment. Testing this notion, Figure 7 shows the calculated C_M from visible video images as a function of the laser light-extinction coefficient. The value of C_M is seen to be inversely proportional to the light-extinction coefficient for given smoke conditions – analogous to Eq. 6.

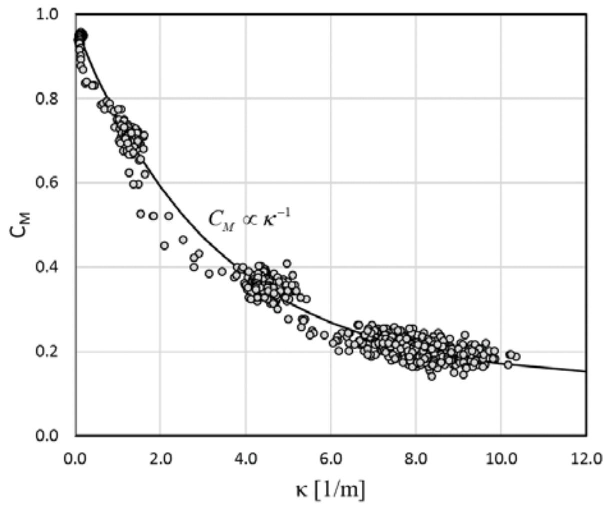

Figure 7. Relationship between the 780 nm laser light-extinction coefficient and the C_M of the acquired visible image through the optical smoke cell.

Figure 8 shows the measured FTIR spectra, with 1 cm^{-1} resolution, of the optical smoke cell content for different smoke obscuration conditions. The sharp lines represent spectral features of key combustion species in the optical smoke cell such as smoke, CO, CO_2, water vapor and unburned gaseous fuel.

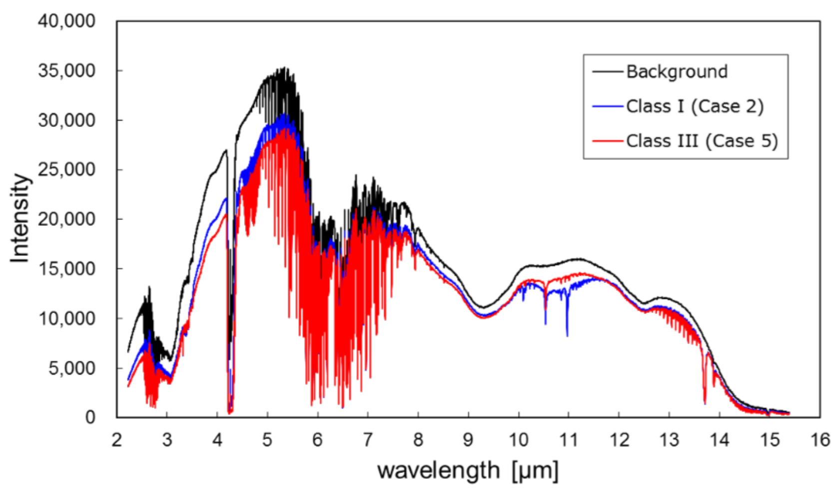

Figure 8. The measured FTIR spectral intensity for different smoke obscuration conditions.

Figure 9 represents the FTIR spectral transmittance of the optical cell contents over a typical, thermal imager, spectral response range of 8 μm to 14 μm for different, smoke-obscuration conditions. The spectral transmittance was greater than 0.8 except for several dips due to the high absorbance of unburned fuel vapor such as propene and acetylene, where the transmittance near 11 µm and 13.7 µm was greatly reduced. The figure also suggests that the concentration of unburned propene was larger for Class I conditions as compared to Class III conditions, when more air was supplied by the chimney burner.

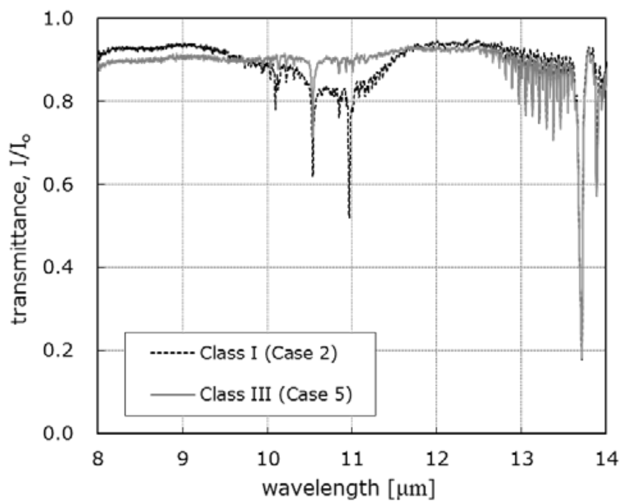

Figure 9. The measured FTIR spectral transmittance for the typical thermal imager spectral response range of 8 µm to 14 µm for different smoke obscuration conditions.

Evaluation of Image Quality through the Smoke Cell

Figure 10 compares the acquired images of the three, thermal imaging, camera technologies for a target temperature of 30 °C and background temperatures of 25 °C, 60 °C, and 100 °C. The smoke obscuration conditions were Class III with light transmission less than 10 %. For the case with a background temperature of 25 °C (When the target temperature was only 5 °C higher than the background), the value of C_M was small. In this case, it was difficult to recognize the bar target due to the small temperature difference between the target and background. TIC A, however, yielded a clearer target image than TICs B or C. For the cases when the target temperature was significantly lower than the background temperature, the value of C_M was relatively large and the target was more clearly recognizable.

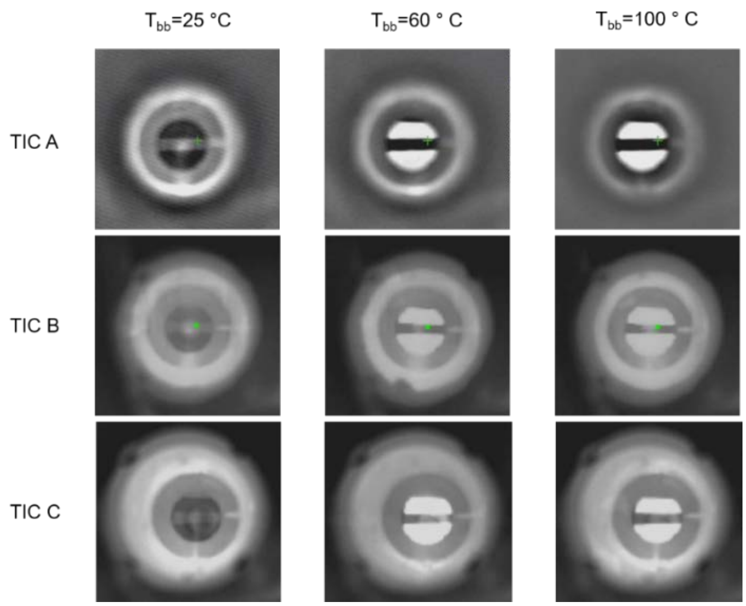

Figure 10. Captured images of three thermal imaging cameras at different background temperatures with a target temperature of 30 °C for the smoke obscuration conditions for Case 5 (Class III).

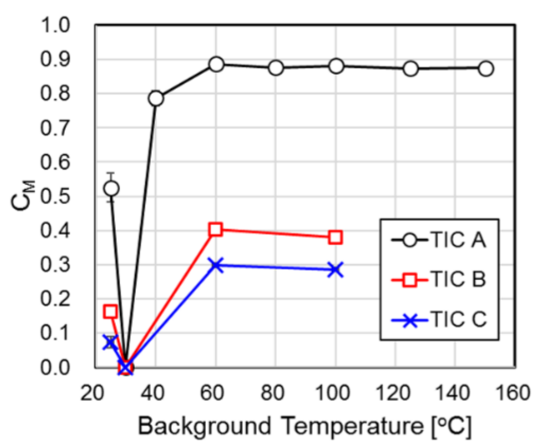

Figure 11. Comparison of the calculated C_M values as a function of background temperature with target temperature held at 30 °C for Class III obscuration conditions (Test 5). A typical uncertainty bar is shown in the figure, representing the combined uncertainty (2σ) for 500 acquired images.

Figure 11 compares the calculated mean C_M values for 500 captured images for the thermal imaging cameras under Class III smoke obscuration conditions. The target temperature was maintained at 30 °C and the background temperature was varied from 25 °C to 150 ºC. The C_M value was determined considering the maximum and minimum measured pixel luminance of the target and background. For the case of a background temperature of 25 °C (lower than the target temperature), the C_M value was relatively low, ranging from 0.1 to 0.5, depending on the specific camera. For background temperatures above 60 °C, the C_M value was about constant.

Figure 12 compares the calculated C_M value of TIC A and TIC B as a function of smoke density for a target temperature of 30 ºC and background temperatures of 25 ºC, 60 ºC, and 100 ºC. For a specific background temperature, the C_M values for TIC A and TIC B were about constant regardless of the smoke density. For TIC A, the C_M value was approximately 0.5 for conditions when the background temperature was lower than the target temperature and about 0.9 for conditions when the background was significantly higher than the target temperature. The C_M values of TIC B were somewhat smaller than TIC A. Measurements showed that the performance of TIC C was very similar to that of TIC B.

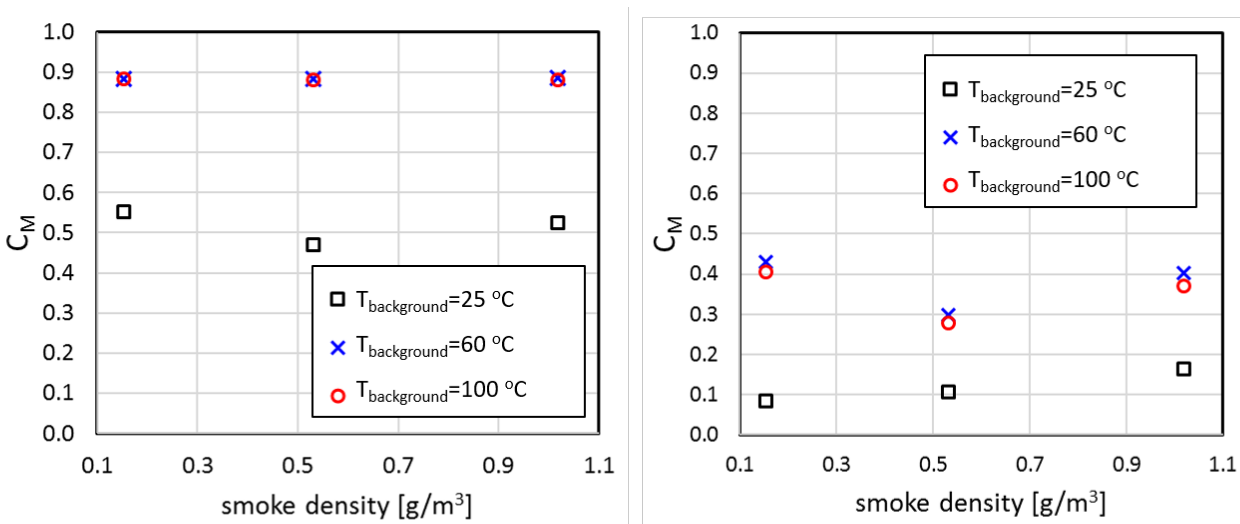

(a) TIC A (b) TIC B

Figure 12. Comparison of the calculated C_M values of TIC A and B as a function of smoke density with target temperature held at 30°C for different background temperature conditions.

Summary and Conclusions

A bench-scale test facility with combustion products (gases and smoke particulates) was utilized to understand key parameters affecting the evaluation of the performance of a thermal imager. The combustion products and smoke concentration inside the optical smoke cell were characterized for different smoke obscuration conditions. The image quality, as measured by the C_M, was examined for various background thermal conditions. The conclusions are summarized below.

- The present study categorized test conditions into three levels based on the transmittance of a 780 nm laser light beam through the optical smoke cell. The measured FTIR spectra of the optical cell for different smoke obscuration conditions showed smoke, CO, CO_2, water vapor and unburned gaseous fuel in the optical smoke cell.
- The overall uniformity of the light-extinction coefficient along the lower and upper parts of the optical smoke cell was about 10 %, which provided a reasonable level of uniformity for testing the performance of thermal imagers.
- The Michelson contrast (C_M) was used to quantitatively characterize imager performance. The C_M value of images captured in the visible through the optical smoke cell has a linear relationship with Jin's visibility function based on light-extinction coefficient measurements, which represents smoke obscuration.
- The measured C_M value from the captured images of thermal imaging cameras were quantitatively compared for different smoke obscuration conditions and thermal conditions of background and target. The absolute C_M value depends mainly on the thermal imager type and the thermal conditions of the background and target. These results represent the inherent characteristics of thermal imagers used in fire service applications, which are less sensitive to obscuring media and more sensitive to thermal conditions than visible cameras.
- For the limited thermal configuration investigated here involving a constant target temperature of 30 °C and background temperature less than 150 °C, measurements showed that the value of C_M depended on the camera type. The measurements also showed that the value of C_M depended on the temperature difference between the target and background, rather than the smoke obscuration conditions in the smoke cell. This implies that contrast can serve as an adequate surrogate for smoke obscuration for the evaluation of imager performance.

Acknowledgements

The authors are indebted to Francine Amon and Joshua Dinaberg for many helpful discussions and technical support during this study.

REFERENCES

[1] Lloyd, J. M, 1975, "Thermal imaging system," Optical Physics and Engineering, Springer.

[2] Rogalski, A., 2000, "Infrared Detectors," Electrocomponent Science Monographs, Vol. 10, CRC.

[3] Scholer, R., 2005, "Assistance to Firefighters Grants: Appealing for Thermal Imagers," Firehouse, Vol. 30, No. 3, pp. 52-54.

[4] Widmann, J. F., and Duchez J., 2004, "The effect of water sprays on fire fighters thermal imagers," Fire Safety Journal, Vol. 39. No. 3, pp. 217-238.

[5] Amon, F., Bryner, N., Lock, A., and Hamins, A., 2008, "Performance Metrics of Fire Fighting Thermal Imaging Cameras – Small- and Full- Scale Experiments", NIST Technical Note 1499.

[6] Holst, G. C., 1998, "Testing and Evaluation of Infrared Imaging System," 2nd Ed., FL and SPIE Optical Engineering Press, Bellingham, WA.

[7] Sudheer, S., and Prabhu, S.V., 2010, "Measurement of Flame Emissivity of Gasoline Pool Fires," Nuclear Engineering and Design 240 (Issue 10), 3474-3480.

[8] Sudheer, S., and Prabhu, S.V., 2012, "Measurement of Flame Emissivity of Hydrocarbon Pool Fires," Fire Technology, 48, 183-217.

[9] de Vries, J., and Tabinowski, R., 2016, "Flame Attenuation Effects on Surface Temperature Measurements Using IR Thermography," Proc. of SPIE Vol. 9861 98610U-1.

[10] NFPA 1801, 2009, "Standard on Thermal Imagers for the Fire Service", National Fire Protection Association.

[11] Amon, F., Hamins, A., 2006, "First responder thermal imagers: development of performance metrics and test methods," Proceedings of SPIE, Vol. 6207.

[12] Chrzanowski, K., 2004, "Testing thermal cameras," IRS2 Conference 2004, Nurnberg, Germany.

[13] Mulholland, G. W., Johnsson, E. L., Fernandez, M. G, and Shear D. A., 2000, "Design and Testing of a New Smoke Concentration Meter," Fire and Materials, Vol. 24, No. 5, pp. 231-243.

[14] Mulholland, G. W., and Croarkin, C., 2000, "Specific Extinction Coefficient of Flame Generated Smoke," Fire and Materials, Vol. 24, No. 5, pp. 227-230.

[15] Michelson, A., 1995, "Studies in Optics," Dover Publications.

[16] Jin, T., 1978, "Visibility through Fire Smoke," Journal of Fire and Flammability, Vol. 9, pp, 135-157.

[17] Mulholland, G. W., 2004, "Chapter 13. Smoke Production and Properties," SFPE Handbook of Fire Protection Engineering, 3rd Edition, 2-265.

[18] Hadjisophocleous, G. V., and Benichou, N., 1999, "Performance criteria used in fire safety design," Automation in Construction, Vol. 8, pp. 489-501.